High-K^+ causes inner hair cell ribbon synapse degeneration

Hong-Bo Zhao, Yan Zhu, Li-Man Liu

Dept. of Otolaryngology, University of Kentucky Medical School, 800 Rose Street, Lexington, KY 40536

Running title: K^+ causes synapse degeneration in the cochlea

Corresponding Author:
Hong-Bo Zhao, Ph.D./M.D.
Professor
Dept. of Otolaryngology
University of Kentucky Medical Center
800 Rose Street
Lexington, KY 40536 – 0293
Tel: 859-257-5097 x 82138
Fax: 859-257-5096
E-mail: hzhao2@uky.edu

Keywords: potassium; ribbon synapse degeneration; BK channel; Glutamate receptor; inner hair cell; auditory nerve; hidden hearing loss; noise-induced hearing loss; age-related hearing loss

Abstract

Recent studies demonstrated that inner hair cell (IHC) ribbon synapses, the first-synapse in the mammal auditory system, could be degenerated by noise and aging, leading to hidden hearing loss (HHL) and eventually other hearing disorders. However, the underlying mechanism remains unclear. Here, we report that elevation of extracellular K^+ could induce IHC ribbon degeneration. Similar to noise-exposure, the degeneration was dose-dependent and only occurred in IHCs. Blockage of Ca^{2+}-dependent K^+ (BK) channels attenuated the degeneration. However, application of the IHC ribbon synapse neurotransmitter glutamate and glutamate receptor (GluR) agonists only caused ribbon swelling but not degeneration; GluR antagonist also had no effect on the regeneration, suggesting that glutamate-excitotoxicity is not a mechanism for ribbon degeneration in IHCs. These data reveal a new presynaptic mechanism for IHC synapse degeneration and HHL, and also suggest that the BK channel is a potential target for prevention and treatment of this common cochlear synaptopathy.

Introduction:

Noise is a common factor for deafness. It has been estimated that more than 100 million people in the United States have noise-induced hearing loss. Recent studies demonstrated that even exposure to moderate levels of noise in a short-term episode, the ribbon synapses between inner hair cells (IHCs) and auditory nerves are extensively degenerated without hair cell loss (*1-4*), therefore leading to hidden hearing loss (HHL) (*2, 5-6*). This cochlear synaptic degeneration could eventually cause impairment in neural adaptation and temporal and speech processing and results in difficulty in hearing speech in noisy environments (*7-9*). Such complains account for ~10% of patients who present to otolaryngology clinics (*7,10*). This cochlear synaptopathy is also associated with early stage of age-related hearing loss and other hearing disorders (*2, 11-14*). However, the underlying mechanism for this cochlear synaptopathy remains unclear.

The ribbon synapses between IHCs and auditory nerves are composed of presynaptic ribbons in IHCs and postsynaptic glutamate receptors (GluR) at auditory nerve endings (Fig. 1A). Glutamate is a major neurotransmitter of this ribbon synapse (*15*). It has been hypothesized that noise exposure may increase glutamate release producing excitotoxicity leading to cell and synapse degeneration (*16-18*). However, GluRs locate at the postsynaptic auditory nerve endings. This glutamate excitotoxicity hypothesis is hard to explain presynaptic ribbon degeneration in hair cells. Moreover, it has been found that despite substantial terminal swelling following perfusion of GluR agonists, the presynaptic and postsynaptic components remained intact (*19,20*). A recent study also demonstrated that ribbon synapses in GluR deficient mice could still be swollen for noise

exposure (*18*). These data suggest that except glutamate-excitotoxicity other mechanisms may also play an important role in ribbon degeneration.

It has been well-known that noise-induced hair cell and auditory nerve excessive-excitation increases intracellular K^+-efflux from hair cells and auditory nerve endings, thereby leading to elevation of extracellular K^+ concentration. Also, noise could impair the reticular lamina integrity and the endolymph-perilymph barrier allowing K^+-rich endolymph (K^+ =~150 mM) entering the perilymph to elevate extracellular K^+ concentration around hair cells producing K^+-toxicity (*21, 22*). In this study, we found that high-K^+ could cause IHC ribbon degeneration. The degeneration could be attenuated by K^+ channel blockers. However, glutamate and GluR agonists could cause ribbon swelling but not degeneration. These data demonstrated that K^+-excitotoxicity rather than glutamate-excitotoxicity plays a central role in the IHC ribbon synapse degeneration in HHL. These data also shed light on the prevention and treatment of the cochlear synaptopathy and HHL.

Results:

Degeneration of IHC ribbons by high-K^+

Fig. 1 shows that high extracellular K^+ caused IHC ribbon degeneration. After challenge with 50 mM K^+ for 2 hr, the ribbon numbers in IHCs were significantly reduced from 14.9±0.81 /IHC in the control group, which was incubated with NES for 2 hr, to 7.55±0.52/IHC (P=1.66E-5, paired t test, two-tail) in the high-K^+ group; the IHC ribbons were reduced by ~50% (Fig. 1D-G). High-K^+ also caused ribbon swollen (Fig. 1E). In comparison with that in control group, the ribbon volume in the high-K^+ group was increased by 1.80±0.22 fold (Fig. 1G, P=0.003, paired t test, two-tail). We further examined the effect of incubation procedure on the ribbon swelling and degeneration (Fig. S1). The numbers of ribbons in the non-incubation group, in which the inner ears were immediately fixed for immunofluorescent staining after isolation, were 12.3±0.96/IHC and had no significant change in comparison with 12.3±1.01/IHC in the incubation of NES incubation for 2 hr (Fig. S1C) (P=0.98, pared t test, two-tail). However, the average volumes of ribbons in the non-incubation group and in the incubation group were 0.520±0.037 and 0.683±0.048 μm^3, respectively (Fig. S1D); the ribbon volumes in the incubation group were significantly increased by 31.3% (P=0.002, paired t test, two-tail).

Fig. 1

K^+-induced ribbon degeneration is dose-dependent (Fig. S2). As extracellular K^+ concentration increased, the ribbon degeneration was increased. When the extracellular

K^+-concentration was greater than 30 mM, the ribbon degeneration reached a stable stage level. The median concentration of K^+ was at 24.7 mM.

Elimination of ribbon degeneration by Ca^{2+}-dependent K^+ channel blockers

To further test whether K^+-excitotoxicity causes ribbon degeneration, we added a Ca^{2+}-dependent K^+ channel blocker tetraethylammonium (TEA) in the high-K^+ (50 mM) incubation solution. Fig. 2 shows that TEA could significantly attenuate K^+ induced ribbon degeneration. With 20 mM TEA, 82.2±1.85% of IHC ribbons was reserved for high-K^+ challenge in the high-K^++TEA group (Fig. 2C). In comparison with the degeneration in the high-K^+ group, the ribbon degeneration in the high-K^++TEA group was significantly reduced by 63.8% (P=0.01, paired t test, two-tail). However, the ribbon swelling was not reduced. In comparison with that in NES group, the ribbons in the high-K^+ group and high-K^++TEA group were swollen by 1.80±0.18 and 1.80±0.20 fold, respectively (Fig. 2D). There was no significant difference between these two groups (P=0.95, paired t test, two-tail).

Fig. 2

We also used Co^{++} to block Ca^{++} channels and Ca^{++}-dependent K^+ channels. Application of Co^{++} (2 mM) significantly reduced high-K^+ induced IHC ribbon degeneration and swelling (Fig. 2E-H). The ribbon survival was increased from 50.8±7.00% in the control high-K^+ group to 72.7±7.07% in the high-K^++Co^{++} group (Fig. 2G, P=0.006, paired t test, two-tail), increased by 44.5%. Co^{++} also significantly

eliminated ribbon swelling (Fig. 2H). The ribbon in the high-K^+ group were swollen by 1.80±0.16 fold in comparison with that in the NES control group and were reduced to 1.29±0.14 fold in the high-K^++Co^{++} group (Fig. 2H, P=0.005, paired t test, two-tail), reduced by 63.8%.

Fig. 3

Fig. 3 shows that extracellular ionic blocking solution (EIBS), which contains 20 mM TEA, 2 mM Co^{++}, and 20 mM Cs^+, to block both K^+ and Ca^{++} channels, could almost completely eliminate ribbon degeneration. In the high-K^++EIBS group, 95.5±3.0% of IHC ribbons were reserved, i.e., only 4.5% of ribbons were degenerated for 50 mM K^+ challenge (Fig. 3A, P=0.002, paired t test, two-tail). The survival of the ribbon number in the high-K^++EIBS group was significantly increased in comparison with that in the high-K^++Co^{++} group but was not significantly changed in comparison with that in the high-K^++TEA group (Fig. 3C, P=0.008 and 0.193, respectively, one-way ANOVA with a Bonferroni correction). The ribbon swelling in the high-K^++EIBS group was also reduced to 1.24±0.17 fold (Fig. 3B) and was significantly reduced by 70.0% (P=0.0007, paired t test, two-tail), similar to the reduction in sole Co^{++} treatment (Fig. 3D, P=1.00, one-way ANOVA).

Glutamate receptor agonists can cause ribbon swelling but not degeneration

However, IHC ribbons were not reduced by application of high-concentration of GluR agonists. Fig. 4 shows that application of GluR agonist glutamate (0.2 mM), KA

(0.3 mM) or NMDA (0.3 mM) did not produce apparent ribbon degeneration. In comparison with that in the control cochlea with normal NES incubation, 97.4±3.90%, 97.4±8.56%, and 101.4±10.2% of IHC ribbons were reserved after treated with glutamate, KA, and NMDA, respectively (Figs. 4C,E,G). There were no significant differences between control and treated groups (Figs. 4C,E,G; P=0.55, 0.70, and 0.83, respectively, paired t test, two-tail). However, GluR agonists could cause ribbon swelling (Figs. 4D,F,H). In comparison with that in the control ears, the volume of ribbons in groups treated with glutamate, KA, or NMDA was significantly increased by 2.08±0.15, 1.65±0.20, and 1.75±0.24 fold, respectively (P=0.0002, 0.01, and 0.04, respectively, paired t test, two-tail).

Fig. 4

GluR antagonists also could not eliminate high-K^+ induced ribbon degeneration and swelling (Fig. 5). Application of a GluR antagonist cyanquixaline (CNQX, 0.1 mM) had no significant effect on the K^+-induced ribbon degeneration and swelling. There were no significant differences in ribbon numbers and volumes between the high-K^+ group and the CNQX+high-K^+ group (P=0.05 and 0.25, respectively, paired t test, two-tail).

Fig. 5

Noise-induced ABR threshold shift and cochlear ribbon synapse degeneration

We further examined the ribbon synapse degeneration after exposure to noise. Fig. 6 shows ABR threshold shift and the cochlear ribbon degeneration after exposure to white

noise (95dB SPL) for 2 hr. The ABR thresholds were significantly increased after noise-exposure (Fig. 6A&B). Before noise exposure, there were no significant differences in ABR thresholds between control and noise-exposure groups (Fig. 6A). ABR thresholds were 22.0±0.5, 22.3±1.08, 14.5±1.38, 19.5±0.82, 25.3±0.58, and 28.3±1.06 dB SPL in control group and 21.3±0.67, 19.3±2.04, 11.0±1.45, 16.0±1.55, 22.0±1.04, and 27.0±2.41 dB SPL in noise-exposure groups for click, 8, 16, 24, 32, and 40 kHz tone stimulations, respectively. After noise exposure, ABR thresholds in the noise-exposed mice were 59.0±1.83, 52.7±3.40, 61.0±2.17, 67.3±1.95, 67.3±3.75, and 67.5±4.35 dB SPL for click, 8, 16, 24, 32, and 40 kHz tone stimulations, respectively ($P< 0.001$, one-way ANOVA with a Bonferroni correction). The ABR thresholds in noise-exposure group were increased by ~ 40 to 50 dB SPL (Fig. 6B). Immunofluorescent staining (Fig. 6C) shows that IHC ribbons were apparently reduced after noise exposure. The ribbon number in noise-exposure mice was 8.97±0.62 per IHC (Fig. 6D). In comparison with 13.9±0.34 per IHC in control mice, the ribbon numbers in the noise-exposure mice were significantly reduced by 35.5% ($P< 0.001$, one-way ANOVA with a Bonferroni correction).

Fig. 6

Moreover, both noise-exposure and high-K+ challenge only caused IHC ribbon degeneration but not outer hair cell (OHC) degeneration (Fig. S3). The OHC ribbons in the control group and high-K^+ (50 mM) group were 2.40±0.04 and 2.43±0.04 per OHC, respectively (Fig. S3C). There is no significant difference between them ($P= 0.31$, paired t test, two-tail). In addition, there is no significant difference in OHC ribbons between

noise-exposure and control groups (Fig. S3D-F). The OHC ribbons in the control group and noise-exposure group were 2.38±0.05 and 2.47±0.04 per OHC, respectively (P=0.25, t test, two-tail).

Discussion:

The ribbon is the structural hallmark of IHC afferent synapses in the cochlea. In this study, we found that high-K^+ could cause IHC synaptic ribbon degeneration and swelling (Fig. 1). Similar to noise exposure induced hearing loss and ribbon synapse degeneration, the K^+-induced ribbon degeneration was dose-dependent (Fig. S2). K^+ channel blockers could attenuate ribbon degeneration but not swelling, while Ca^{++} channel blockers could attenuate both ribbon degeneration and swelling (Figs. 2&3). However, GluR agonists could cause ribbon swelling but not degeneration (Fig. 4). Application of the GluR antagonist CNQX also had no effect on high-K^+ induced ribbon degeneration (Fig. 5). Finally, the K^+-toxicity induced ribbon degeneration was similar to the noise-induced cochlear synaptopathy, and only occurred in IHCs but not in OHCs (Figs. 6&S3). These data indicate that noise-induced K^+-excitotoxicity plays a critical role in the presynaptic ribbon degeneration in IHCs in HHL.

As mentioned above, it has been hypothesized that the ribbon synapse degeneration may result from glutamate excitotoxicity, i.e., acoustic overstimulation (noise exposure) induces excessive glutamate release leading to ribbon synapse excitotoxicity and degeneration (*17)*. However, GluRs mainly locate at the postsynaptic auditory nerve endings. It is hard to explain glutamate excitotoxicity to cause presynaptic ribbon degeneration. Previous experiments also demonstrated that the presynaptic and postsynaptic components remained intact after perfusion of GluR agonists (*19,20*). In addition, a recent study demonstrated that ribbon synapses in GluR deficient mice could still be swollen for noise exposure (*18*). In this study, we found that application of GluR

agonists could cause ribbon swelling but not degeneration (Fig. 4). Application of GluR antagonist also had no effect on ribbon degeneration (Fig. 5). These results suggest that glutamate-induced excitotoxicity is unlikely to be the main mechanism for presynaptic ribbon degeneration.

In this study, we found that high-extracellular K^+ caused IHC ribbon degeneration (Figs. 1-3). The degeneration was dose-dependent and increased as K^+-concentration was increased (Fig. S2). Also, the IHC ribbon degeneration could be blocked by K^+ channel blockers but not GluR antagonist (Figs. 2, 3, 5). These data evidence that K^+ excitotoxicity plays a central role in the ribbon synapse degeneration. This study also provides new important information for developing preventive and therapeutic interventions for ribbon degeneration. We found that K^+ channel blockers could attenuate ribbon degeneration but not swelling (Figs. 2A-D and 3), while Ca^{++} channel blocker Co^{++} could attenuate both ribbon degeneration and swelling (Figs. 2E-H and 3). This may be due to Co^{++} can block Ca^{++} channels and consequently block Ca^{++}-dependent K^+ channels, such as BK channels, which predominantly express at the adult IHCs (*23*,*24*). Indeed, it was found that deficiency of BK channels could increase resistance to noise-induced hearing loss (*24*). This is consistent with our finding that TEA and Ca^{++} channel blocker could attenuate ribbon degeneration (Figs. 2&3). Taken together, these data indicate that K^+ degenerates ribbon synapses in IHCs by K^+-excitotoxicity through BK channel activity. These data also suggest that BK channels may be valuable targets for prevention and treatment of ribbon degeneration in HHL.

These data also reveal that ribbon degeneration and swelling may involve different mechanisms. As shown by the fact that blockage of Ca^{++} channels rather than K^+ channels attenuated ribbon swelling (Figs. 2&3), Ca^{++} may play an important role in ribbon swelling and K^+ excitotoxicity may play a critical role in ribbon generation. This concept is consistent with previous reports that GluR agonists could cause ribbon swelling (*20, 25-27*), due to GluRs are permeable to Ca^{++}. Activation of GluRs can induce Ca^{++} influx, which may lead to ribbon swelling but not degeneration (Fig. 4).

IHC synapse area is embedded in the perilymph. K^+-level in the perilymph is normally as low as in the extracellular space. However, when the sensory cells and neurons are excited, they will release K^+ from intracellular to the perilymph, which could increase perilymph K^+-concentration. The K^+-concentration in the local extracellular space around hair cells could be even higher. Noise, aging or other factors also could impair the reticular lamina integrity and the endolymph-perilymph barrier allowing K^+-rich endolymph (K^+ =~150 mM) entering the perilymph (*21, 22*). High-extracellular K^+ could produce excitotoxicity. It has been reported that high-extracellular K^+ following neuron damages and injury by stroke in the brain could cause secondary cell death in the neighboring area (*28, 29*). In this study, we found that high-extracellular K^+ caused IHC ribbon degeneration (Figs. 1-3). The degeneration was increased as K^+-concentration was increased (Fig. S2), similar to intensity-dependence of ribbon synapse degeneration for noise exposure (*30*). Moreover, as observed ribbon synapse degeneration in HHL by noise exposure, K^+ excitotoxicity only causes IHC ribbon degeneration but not OHC ribbon degeneration (Fig. S3). These data indicate that K^+ excitotoxicity may play a

central role in the noise-induced cochlear synapse degeneration in the HHL.

Our previous study demonstrated that ATP-P2X purinergic receptors are required for sinking K^+ to reenter into cells in the cochlea (*31*). P2X2 is a predominant P2X receptor in hair cells and supporting cells in the cochlea. P2X2 mutation can increase susceptibility to noise and induce hearing loss (*32*). P2X2 receptors also have been found to be necessary for the development of noise-induced temporal threshold shift (*33*). These studies further support the concept that K^+-toxicity may play a critical role in noise-induced cochlear synaptopathy.

This study also provides important information for mechanisms underlying other cochlear and hearing disorders, such as Meniere's disease. It is well-known that K^+-toxicity plays a central role in Meniere's disease. Its symptoms have been considered to be K^+ intoxicating the hair cells and nerve fibers in the perilymph (*34,35*). In this study, we found that high-K^+ could cause IHC ribbon degeneration (Figs. 1&2). Indeed, it was found that there was a significant decrease in the number of afferent nerve endings and afferent synapses at the base of both inner and outer hair cells in the ear with Meniere's disease (*36*). Our finding, therefore, may also provide important information for understanding mechanisms underlying Meniere's disease.

Finally, our finding that K^+ excitotoxicity causes IHC ribbon degeneration may also shed light on mechanisms for age-related hearing loss. It has been reported that age-related hearing loss has apparent IHC ribbon synapse degeneration in the cochlea (*2, 11,*

12, 14). As mentioned above, cell degeneration could release K^+ and increase extracellular K^+ concentration. Age-induced hair cell and SG neuron or auditory nerve degenerations could release K^+ and increase local K^+ concentration, which could lead to more extensive ribbon degeneration in neighboring cells in aged-ears, like the secondary cell death following stroke in the brain (*28*,*29*).

Materials and Methods:

Animal and cochlear preparations

Both genders of adult CBA/CaJ mice (8-12 weeks old, Stock No: 000654, The Jackson Lab) were used. Mice were housed in a quiet individual room in basement with regular 12/12 light/dark cycle. The background noise level in the mouse room at mouse hearing range (4-70 kHz) is <30 dB SPL. All procedures and experiments followed in the use of animals were approved by the University of Kentucky's Animal Care & Use Committee (UK: 00902M2005) and conformed to the standards of the NIH Guidelines for the Care and Use of Laboratory Animals.

Cochlear preparation and high-K^+ challenge

The mouse cochlea was freshly isolated and the temporal bone was removed. The otic capsule was opened. The round window membrane was broken by a needle and a small hole was also made at the apical tip of the cochlea. The left or right cochlea was randomly selected and incubated in the high-K^+ solution or other solutions; another cochlea in the same mouse was simultaneously incubated in the normal extracellular solution (NES) or other control solutions. At the beginning of incubation, the gent suctions and blows on the round window and the apical hole were performed for several times to ensure the incubation solution quickly entering into the cochlea. The complete exchange of perilymph could be verified with solution fluxed out of the round window or the apical hole by eyes under a stereo microscope (SMZ745, Nikon). After incubation for 2 hr, both the treated cochlea and the control cochlea were immediately fixed with 4% paraformaldehyde in PBS for 1 hr.

The normal extracellular solution (NES) was prepared by 142 NaCl, 5.37 KCl, 1.47 $MgCl_2$, 2 $CaCl_2$, 10 HEPES in mM. High-K^+ extracellular solution was prepared by replacement of NaCl with KCl in the NES (*31*). The high-glutamate solution was made by adding 0.2 mM L-glutamate (cat. #49621, Sigma-Aldrich Inc) into the NES. The extracellular ionic blocking solution (EIBS) was prepared by 100 NaCl, 20 tetraethylammonium (TEA), 20 CsCl, 2 $CoCl_2$, 1.47 $MgCl_2$, 2 $CaCl_2$, 10 HEPES in mM (Yu and Zhao, 2008). Other incubation solutions were prepared by description in the text. All solutions were adjusted to pH 7.2 and 300 mOsm. The osmolality was verified by a freezing pressure micro-osmometer (Model 3300, Advance Instrument). Chemicals were purchased from Sigma-Aldrich Inc. (St. Louis, MS, USA). NMDA, Kainic acid (KA), and CNQX (6-cyano-7-nitroquinoxaline-2,3-dione) were purchased from TOCRIS Bioscience (cat. #0114, 0222, and 1045, respectively).

Histological preparations for staining

After fixation, the cochlea was dissected as reported in our previous publications (*37,38*). Under a stereo microscope (SMZ745, Nikon), the bone enclosed the cochlea was gently crashed and removed. Then, the tectorial membrane and stria vascularis were carefully torn off by a fine forceps. The basilar membrane with the organ of Corti (auditory sensory epithelium) was picked away by a sharpened needle and collected for staining. Since the sensory epithelium in the basal turn in mice is very difficultly dissected, the isolated sensory epithelia for immunofluorescent staining in the most cases in this study were come from the apical and middle turns.

Immunofluorescent staining and confocal microscopy

Both of the treated cochlea and the control cochlea in the same mouse were stained in parallel to minimize variations of the performance. As described in our previous reports (*39*), the isolated cochlear sensory epithelia were incubated in a blocking solution (10% goat serum and 1% BSA of PBS) with 0.1% Triton X-100 for 30 min. Then, the epithelia were incubated with primary antibodies for CtBP2 (1:200, mouse anti-CtBP2 IgG1, #612044, BD Bioscience) or with mouse anti-Glue2 IgG2a (1:1000, #MAB397, Millipore Corp.) in the blocking solution at 4ºC overnight. After washout, the epithelia were incubated with corresponding second Alexa Fluor antibodies (1:400, goat anti-mouse IgG1 Alexa Fluor 568, A-21124, or with goat anti-mouse IgG2a Alexa Fluor 488, A-21131, Thermo Fisher Sci) at room temperature (23 ºC) for 2 hr. Before washout, 4', 6-diamidino-2-phenylindole (DAPI, 50 μg/ml, D1306; Thermo Fisher Sci) was added to visualize the cell nuclei. After incubation for 2 min, the sensory epithelia were washed by PBS for 3 times and whole-mounted on the glass-slide.

The stained epithelia were observed under a Nikon A1R confocal microscope system. Machine cross-talking was checked by the standard fluorescent slides and turn-on/off of one laser in dual-laser excitation. No cross-talk was observed. In each cochlea, at least 5 fields were scanned along the cochlear sensory epithelium from the apical to the basal. In each field, serial sections were taken along the Z-axis from the bottom to apical surface of the epithelium with a 0.25 μm step. All fluorescence microscopy was imaged using a Nikon 100x (N/A: 1.45) Plan Apro oil objective at 0.25 μm/pixel resolution.

Quantitative analysis and image presentation

For ribbon number accounting, the maximum intensity projection was generated from z-stack images. The numbers of CtBP2 labeling in the IHC region and the OHC region were separately accounted by NIS Elements AR Analysis software (Nikon). The ribbon number per IHC or OHC in the each field of view was calculated and then averaged among the observed fields in the each cochlea.

The ribbon volumes were measured by Imaris software (Bitplane Inc., MA, USA). The 3D-image was created from z-stack sections. The cell-vesicle volume function was selected with 0.15 μm smoothing. The volume measurement was performed by defining a minimum threshold above local background and a minimum acceptable Guissian distribution of voxel intensity to minimize false-positive noise. Similar parameters were used among mice. The volumes of IHC ribbons in at least 3 different fields of view in each cochlea were measured and averaged. The measured ribbon volume was normalized to that in the control ear in the same animal and further averaged among different animals within a given experiment (*40*).

Noise exposure

To ensure age and sex-matched control, mice in one cage were randomly separated to noise exposure group and control group. For noise exposure, mice were awake in a small cage under loud-speakers in a sound-proof chamber and exposed to white-noise (95-98 dB SPL) for 2 hr, one time. Sound pressure level and spectrum in the cage were measured prior to placement of the animal.

Auditory brainstem response recording

Auditory brainstem response (ABR) was recorded by use of a Tucker-Davis R3 workstation with ES-1 high frequency speaker (Tucker-Davis Tech. Alachua, FL) (*37,38*). ABR was recorded by stimulation with clicks in alternative polarity and tone bursts (4-40 kHz) from 80 to 10 dB SPL in a 5 dB step in a double-walled sound isolation room. The signal was amplified (50,000x), filtered (300-3,000 Hz), and averaged by 500 times. The ABR threshold was determined by the lowest level at which an ABR can be recognized. ABR was recorded at 1-2 day before noise exposure as reference and immediately after noise exposure to assess the threshold shift.

Statistical analysis

Data were plotted by SigmaPlot and statistically analyzed by Excel (Microsoft Office) or SPSS (SPSS Inc.; Chicago, IL). Error bars represent SEM. Parametric and nonparametric data comparisons were performed using one-way ANOVA or Student t tests after assessment of normality and variance (SigmaPlot v13, Systat Software, or SPSS, SPSS Inc). We compared measures within the same group using the pared, two-tailed Student's t test. The threshold for significance was $\alpha = 0.05$. ANOVAs used Bonferroni *post hoc* test.

Acknowledgement:

This work was supported by NIH R01 DC 017025, DC 017025-01S1, and R56 DC 016585 to HBZ.

Author Contributions:

HBZ conceived the general framework of this study. YZ, LML and HBZ performed the experiments. HBZ and YZ analyzed data. HBZ wrote the paper. All authors reviewed the manuscript and provided the input.

Conflict of Interest:

The authors declare no competing financial interests.

Data and materials availability: All data needed to evaluate the conclusions in the paper are present in the paper and/or the Supplementary Materials. Additional data related to this paper may be requested from the authors.

References:

1. Kujawa SG, Liberman MC. (2009) Adding insult to injury: cochlear nerve degeneration after "temporary" noise-induced hearing loss. J Neurosci. 29: 14077-14085.

2. Kujawa SG, Liberman MC. (2015) Synaptopathy in the noise-exposed and aging cochlea: Primary neural degeneration in acquired sensorineural hearing loss. Hear Res. 330: 191-199.

3. Lin HW, Furman AC, Kujawa SG, Liberman MC. (2011) Primary neural degeneration in the guinea pig cochlea after reversible noise-induced threshold shift. J Assoc Res Otolaryngol. 12: 605-616.

4. Furman AC, Kujawa SG, Liberman MC. (2013) Noise-induced cochlear neuropathy is selective for fibers with low spontaneous rates. J Neurophysiol. 110: 577-586. doi: 10.1152/jn.00164.2013.

5. Moser T, Starr A. (2016) Auditory neuropathy--neural and synaptic mechanisms. Nat Rev Neurol. 12: 135-149. doi: 10.1038/nrneurol.2016.10.

6. Boero LE, Castagna VC, Di Guilmi MN, Goutman JD, Elgoyhen AB, Gómez-Casati ME. (2018) Enhancement of the medial olivocochlear system prevents hidden hearing loss. J Neurosci. 38: 7440-7451. doi: 10.1523/JNEUROSCI.0363-18.2018.

7. Kumar U, Ameenudin S, Sangamanatha A. (2012) Temporal and speech processing skills in normal hearing individuals exposed to occupational noise. Noise Health. 14:100.

8. Plack CJ, Barker D, Prendergast G. (2014) Perceptual consequences of "hidden" hearing loss. Trends Hear. 18: 1-11. pii: 2331216514550621. doi: 10.1177/2331216514550621.

9. Bakay WMH, Anderson LA, Garcia-Lazaro JA, McAlpine D, Schaette R. (2018) Hidden hearing loss selectively impairs neural adaptation to loud sound environments. Nat Commun. 9(1):4298. doi: 10.1038/s41467-018-06777-y.

10. Hind S, Haines-Bazrafshan R, Benton C, Brassington W, Towle B, Moore D. (2011) Prevalence of clinical referrals having hearing thresholds within normal limits. Int J Audiol. 50:708-716.

11. Sergeyenko Y, Lall K, Liberman MC, Kujawa SG. (2013) Age-related cochlear synaptopathy: an early-onset contributor to auditory functional decline. J Neurosci. 33: 13686-13694. doi: 10.1523/JNEUROSCI.1783-13.2013.

12. Viana LM, O'Malley JT, Burgess BJ, Jones DD, Oliveira CA, Santos F, Merchant SN, Liberman LD, Liberman MC. (2015) Cochlear neuropathy in human presbycusis: Confocal analysis of hidden hearing loss in post-mortem tissue. Hear Res. 327:78-88. doi: 10.1016/j.heares.2015.04.014.

13. Kujawa SG, Liberman MC. (2006) Acceleration of age-related hearing loss by early noise exposure: evidence of a misspent youth. J Neurosci. 26: 2115-2123.

14. Parthasarathy A, Kujawa SG. (2018) Synaptopathy in the aging cochlea: Characterizing early-neural deficits in auditory temporal envelope processing. J Neurosci. 38: 7108-7119. doi: 10.1523/JNEUROSCI.3240-17.2018.

15. LePrell CG, Bledsoe SC, Bobbin RP, Puel JL (2001). Neurotransmission in the inner ear: functional and molecular analysis. In: Jahn, A.F., Santos-Sacchi, J. (Eds.), Physiology of the Ear, 2nd edn. Singular Publishing Group, San Diego, CA, pp. 575-611.

16. Puel JL, Ruel J, Gervais d'Aldin C, Pujol R. (1998) Excitotoxicity and repair of cochlear synapses after noise-trauma induced hearing loss. Neuroreport. 9: 2109-2114.

17. Liberman MC, Kujawa SG. (2017) Cochlear synaptopathy in acquired sensorineural hearing loss: Manifestations and mechanisms. Hear Res. 349:138-147.

18. Kim KX, Payne S, Yang-Hood A, Li SZ, Davis B, Carlquist J, V-Ghaffari B, Gantz JA, Kallogjeri D, Fitzpatrick JAJ, Ohlemiller KK, Hirose K, Rutherford MA. (2019) Vesicular Glutamatergic Transmission in Noise-Induced Loss and Repair of Cochlear Ribbon Synapses. J Neurosci. 39: 4434-4447. doi: 10.1523/JNEUROSCI.2228-18.2019.

19. Puel JL, Pujol R, Ladrech S, Eybalin M. (1991) Alpha-amino-3-hydroxy-5-methyl-4-isoxazole propionic acid electrophysiological and neurotoxic effects in the guinea-pig cochlea. Neuroscience. 45: 63-72.

20. Sebe JY, Cho S, Sheets L, Rutherford MA, von Gersdorff H, Raible DW. (2017) Ca^{2+} permeable AMPARs mediate glutamatergic transmission and excitotoxic damage at the hair cell ribbon synapse. J Neurosci. 37: 6162-6175.

21. Konishi T, Salt AN. (1980) Permeability to potassium of the endolymph-perilymph barrier and its possible relation to hair cell function. Exp Brain Res. 40: 457-463.

22. Zenner HP, Reuter G, Zimmermann U, Gitter AH, Fermin C, LePage EL. (1994) Transitory endolymph leakage induced hearing loss and tinnitus: depolarization, biphasic shortening and loss of electromotility of outer hair cells. Eur Arch Otorhinolaryngol. 251: 143-153.

23. Pyott SJ, Duncan RK. (2016) BK Channels in the Vertebrate Inner Ear. Int Rev Neurobiol. 128: 369-399. doi: 10.1016/bs.irn.2016.03.016.

24. Pyott SJ, Meredith AL, Fodor AA, Vázquez AE, Yamoah EN, Aldrich RW. (2007) Cochlear function in mice lacking the BK channel alpha, beta1, or beta4 subunits. J Biol Chem. 282: 3312-3324.

25. Ruel J, Wang J, Rebillard G, Eybalin M, Lloyd R, Pujol R, Puel JL. (2007) Physiology, pharmacology and plasticity at the inner hair cell synaptic complex. Hear Res. 227: 19-27.

26. Sheets L. (2017) Excessive activation of ionotropic glutamate receptors induces apoptotic hair-cell death independent of afferent and efferent innervation. Sci Rep. 7:41102. doi: 10.1038/srep41102.

27. Kim J, Xia A, Grillet N, Applegate BE, Oghalai JS. (2018) Osmotic stabilization prevents cochlear synaptopathy after blast trauma. Proc Natl Acad Sci USA. 115: E4853-E4860. doi: 10.1073/pnas.1720121115.

28. Deshpande LS, Limbrick DD Jr, Sombati S, DeLorenzo RJ. (2007) Activation of a novel injury-induced calcium-permeable channel that plays a key role in causing extended neuronal depolarization and initiating neuronal death in excitotoxic neuronal injury. J Pharmacol Exp Ther. 322: 443-452.

29. Walsh JG, Muruve DA, Power C. (2014) Inflammasomes in the CNS. Nat Rev Neurosci. 15:84-97. doi: 10.1038/nrn3638.

30. Hill K, Yuan H, Wang X, Sha SH. (2016) Noise-induced loss of hair cells and cochlear synaptopathy are mediated by the activation of AMPK. J Neurosci. 36: 7497-7510. doi: 10.1523/JNEUROSCI.0782-16.2016.

31. Zhu Y, Zhao HB. (2010) ATP-mediated potassium recycling in the cochlear supporting cells. Purinergic Signal. 6: 221-229.

32. Yan D, Zhu Y, Walsh T, Xie DH, Yuan HJ, Sirmaci A, Fujikawa T, Wong ACY, Loh TL, Du LL, Grati M, Vlajkovic SM, Blanton S, Ryan AF, Chen ZY, Thorne PR, Kachar B, Tekin M, Zhao HB, Housley GD, King MC, Liu XZ. (2013) Mutation of the ATP-gated P2X2 receptor leads to progressive hearing loss and increased susceptibility to noise. Proc. Natl. Acad. Sci. USA, 110: 2228-2233.

33. Housley GD, Morton-Jones R, Vlajkovic SM, Telang RS, Paramananthasivam V, Tadros SF, Wong AC, Froud KE, Cederholm JM, Sivakumaran Y, Snguanwongchai P, Khakh BS, Cockayne DA, Thorne PR, Ryan AF. (2013) ATP-gated ion channels mediate adaptation to elevated sound levels. Proc Natl Acad Sci USA. 110: 7494-7499.

34. Horner KC. (1993) Review: morphological changes associated with endolymphatic hydrops. Scann Microsc. 7: 223-238.

35. Nakashima T, Pyykkö I, Arroll MA, Casselbrant ML, Foster CA, Manzoor NF, Megerian CA, Naganawa S, Young YH. (2016) Meniere's disease. Nat Rev Dis Primers. 2:16028. doi: 10.1038/nrdp.2016.28.

36. Nadol JB Jr, Thornton AR. (1987) Ultrastructural findings in a case of Menière's disease. Ann Otol Rhinol Laryngol. 96: 449-454.

37. Zhu Y, Liang C, Chen J, Zong L, Chen GD, Zhao HB. (2013) Active cochlear amplification is dependent on supporting cell gap junctions. Nat Commun. 4: 1786 doi: 10.1038/ncommuns2806

38. Mei L, Chen J, Zong L, Zhu Y, Liang C, Jones RO, Zhao HB. (2017) A deafness mechanism of digenic Cx26 (GJB2) and Cx30 (GJB6) mutations: Reduction of endocochlear potential by impairment of heterogeneous gap junctional function in the cochlear lateral wall. Neurobiol Dis. 108: 195-203. doi: 10.1016/j.nbd.2017.08.002.

39. Zhao HB, Yu N. (2006) Distinct and gradient distributions of connexin26 and connexin30 in the cochlear sensory epithelium of guinea pigs. J Comp Neurol. 499:506-518.

40. Yin Y, Liberman LD, Maison SF, LibermanMC (2014) Olivocochlear innervation maintains the normal modiolar-pillar and habenular-cuticular gradients in cochlear synaptic morphology. JARO 15:571–583.

Figure legends:

Fig. 1. High-K^+ causes ribbon degeneration in IHCs. A: Diagram of ribbon synapses between IHC and auditory nerve. B-C: Immunofluorescent staining for ribbon synapses in the IHC area. Presynaptic ribbons are labeled by CtBP2 (red) and postsynaptic Glutamate receptors (GluRs) are labeled by green. Panel C is a high-magnitude image showing presynaptic ribbon labeling and postsynaptic GluR labeling. D-E: Immunofluorescent staining of CtBP2 for ribbons in the IHC area after incubation in the high-K^+ (50 mM) extracellular solution for 2 hr. The control cochlea was simultaneously incubated in the normal extracellular solution (NES). F-G: High-K^+ reduces IHC ribbons and induces ribbon swelling significantly. Dashed lines connected the two same symbols represent that the data were collected from two inner ears in the same mouse. The volume of ribbons in the high-K^+ treated cochlea was normalized to that in the control cochlea of the same mouse. The totally accounted IHCs and measured ribbons are presented within the bars. **: $P<0.01$, paired t test, two-tail. Scale bar: 10 µm in B, D&E; 0.5 µm in C.

Fig. 2. Blockage of Ca^{++}-dependent K^+ channels attenuates ribbon degeneration. A-B: Immunofluorescent staining for CtBP2 after incubation with 50 mM K^+ NES (high-K^+ group) and 50 mM K^+ NES with 20 mM TEA (high-K^++TEA group). Scale bar: 10 µm. C-D: Quantitative analysis of ribbon numbers and swelling after application of TEA for high-K^+ challenge. Ribbon numbers and volumes in the high-K^+ and high-K^++TEA groups are normalized to those in the control group with NES incubation. Dashed lines connected the two same symbols represent that the data were collected from two inner ears in the same mouse. Numbers in the bars represent the total numbers of accounted IHCs and ribbons. E-F: Representative CtBP2 labeling in IHCs in the high-K^+ group and

high-K^+ with 2 mM Co^{++} (high-K^++Co^{++} group). Scale bar: 10 µm. G-H: Quantitative analysis of ribbon numbers and volumes. Ribbon numbers and volumes in both high-K^+ group and high-K^++Co^{++} group are normalized to those in control NES incubation group. Dashed line connections represent data collected from two inner ears in the same mouse. Numbers in the bars represent the total numbers of accounted IHCs and measured ribbons. **: $P < 0.01$, paired t test, two-tail.

Fig. 3. Blockage of Ca^{++} and K^+ channels attenuates K^+-induced IHC ribbon degeneration and swelling. A-B: Extracellular ionic blocking solution (EIBS), which contains TEA (20 mM), Cs^+ (20 mM), and Co^{++} (2 mM), attenuates both of high-K^+ induced ribbon degeneration and swelling. Ribbon numbers and volumes in the high-K^+ group and the high-K^++EIBS group are normalized to those in control NES incubation group. Dashed line connections represent data collected from two inner ears in the same animal treated with high-K^+ and K^++EIBS. Numbers in the bars represent the total numbers of accounted IHCs and measured ribbons. **: $P < 0.01$, paired t test, two-tail. C-D: IHC ribbon survival and volume in the high-K^+ (50 mM) group, high-K^++TEA (20 mM) group, high-K^++Co^{++} (2 mM) group, and high-K^++EIBS group. **: $P < 0.01$, one-way ANOVA with a Bonferroni correction.

Fig. 4. GluR agonists could cause ribbon swelling but not degeneration. A-B: Representative ribbon labeling in IHCs for treatment with high concentration of glutamate (0.2 mM) and the control group with incubation of NES. Scale bar: 10 µm. C-H: Treatments with high-concentration of GluR agonists can cause ribbon swelling but

not degeneration. One cochlea was incubated with NES as control and another cochlea in the same animal was incubated with NES with 0.2 mM glutamate, 0.3 mM kainic acid (KA), or 0.3 mM NMDA. The averaged ribbon number per IHC and ribbon volume were normalized to those in the control NES incubated ear. Dashed line connections represent data collected from two inner ears in the same animal. Numbers in the bar represent the total of IHCs accounted and ribbons measured in each group. There are no significant differences in IHC ribbons between the control groups and the GluR agonist treatment groups. However, ribbon volumes in the GluR agonist groups are significantly increased. **: $P < 0.01$, paired t test, two-tail.

Fig. 5. Application of GluR antagonist has no effect on high-K^+ induced ribbon degeneration and swelling. One cochlea was incubated with 50 mM K^+ NES (high-K^+ group) and another cochlea in the same animal was incubated with 50 mM K^+ NES and 0.1 mM CNQX (high-K^++CNQX group). The averaged ribbon number per IHC and ribbon volume were normalized to those in the control NES incubated ear. Dashed line connections represent data collected from two inner ears in the same mouse. Numbers in the bar represent the total of IHCs accounted and ribbons measured in each group. A: GluR antagonist CNQX cannot eliminate high-K^+ induced ribbon degeneration. B: CNQX cannot attenuate high-K^+ induced ribbon swelling. n.s.: no significance, $P>=0.05$, paired t test, two-tail.

Fig. 6. Noise exposure induced ribbon synapse degeneration. A-B: Noise-induced ABR threshold shift. There was no significant difference in pre-exposure ABR thresholds

between control group and noise exposure group. After noise exposure, the ABR thresholds in the noise-exposure group were significantly increased about 45-55 dB SPL. C-D: Ribbon synapse degeneration in the IHCs after noise exposure. Numbers in the bars represent the total numbers of mice and accounted IHCs. ** $P < 0.001$, one-way ANOVA with a Bonferroni correction. Scale bar: 10 µm.

Fig. S1. Incubation procedure does not produce ribbon degeneration. One inner ear in a mouse was immediately fixed after isolation and stained for CtBP2, while another inner ear in the same mouse was incubated in NES for 2 hr and then fixed for staining. A-B: Immunofluorescent staining for CtBP2 in the immediate control group and NES-incubation group. Scale bar = 10 µm. C-D: Quantitative analysis of ribbon numbers and volumes. Dashed line connections represent data collected from two inner ears in the same mouse. Data were collected from 4 mice. Numbers in the bars represent the total numbers of accounted IHCs and measured ribbons. There is no significant ribbon degeneration after incubation in NES for 2 hr (panel C). However, ribbon volumes in the incubation group are significantly increased (panel D). **: $P < 0.01$, paired t test, two-tail.

Fig. S2. Dose-curve of ribbon degeneration in IHCs by K^+. A smooth solid line represents data fitting to a Hill's function $y=y_0+a*C^n/(EC_{50}^n+C^n)$, where median concentration EC_{50}=24.7 mM .

Fig. S3. No significant ribbon degeneration in outer hair cells (OHCs) for high K^+ challenge and noise exposure. A-B: Immunofluorescent staining for CtBP2 in OHC area for high-K^+ treatment. C: There is no significant degeneration of OHC ribbon synapses for high-K^+ challenge (P=0.31, pared t test, two-tail). D-E: Immunofluorescent staining for CtBP2 in OHC area after noise exposure. F: There is no difference of ribbon synapses in OHCs between noise-exposure group and control group (P=0.25, t test, two-tail). Scale bar = 10 μm.

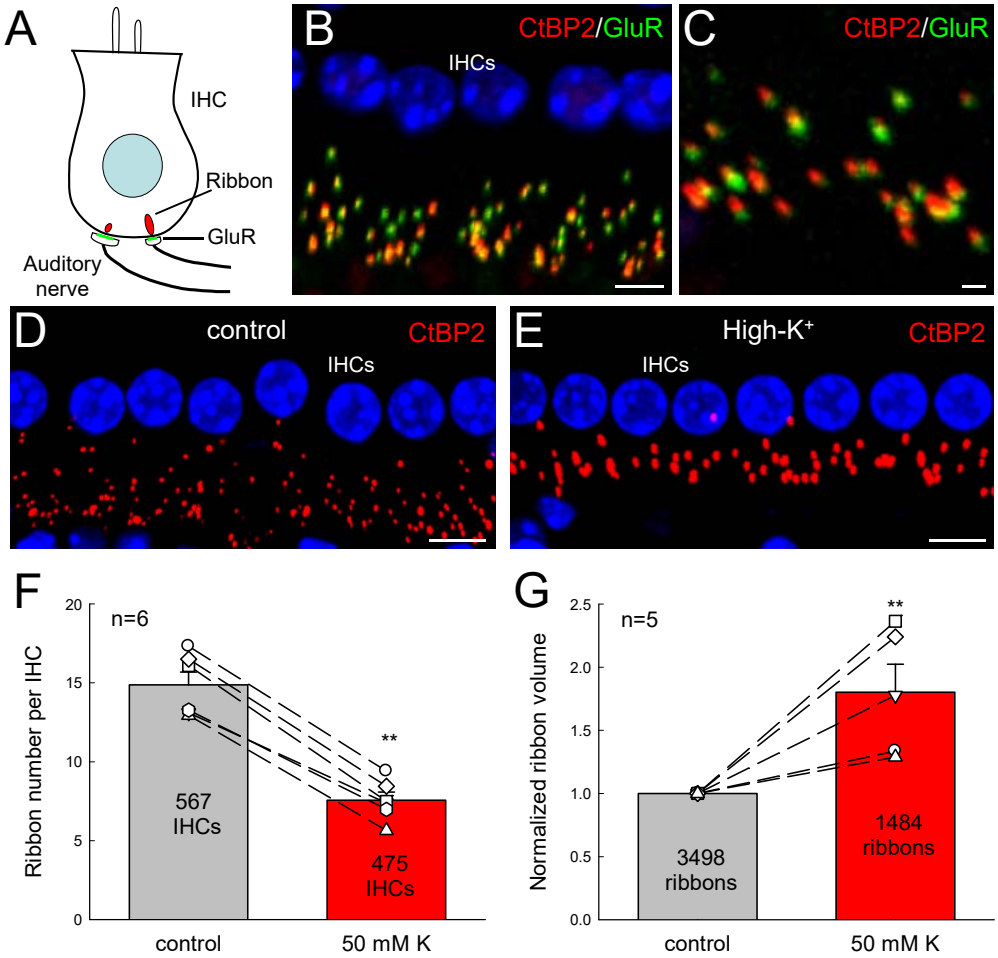

Fig 1. High-K+ induced ribbon degeneration and swelling

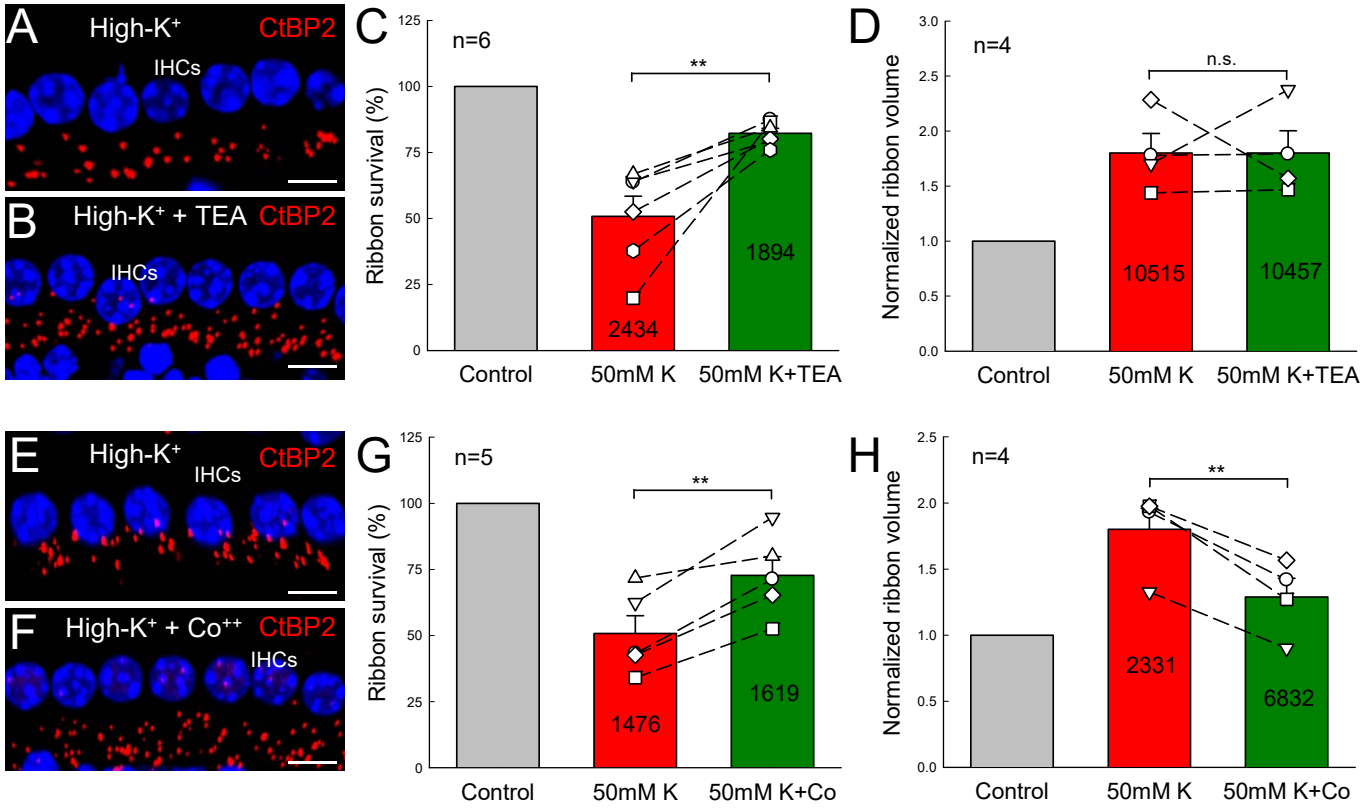

Fig. 2. Attenuation of K^+-induced ribbon degeneration by K^+ and Ca^{++} channel blockers

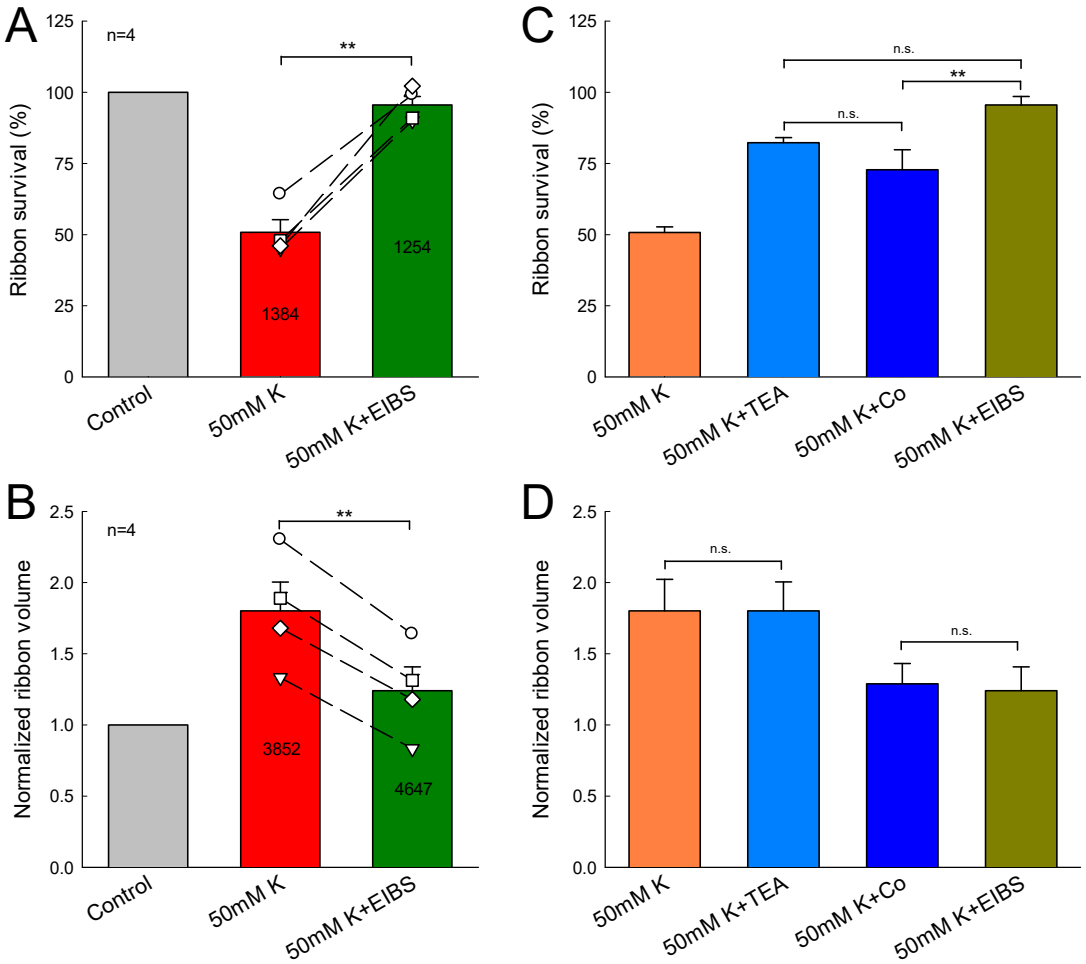

Fig. 3. Blockage of Ca^{++} and K^{+} channels can attenuate ribbon degeneration and swelling

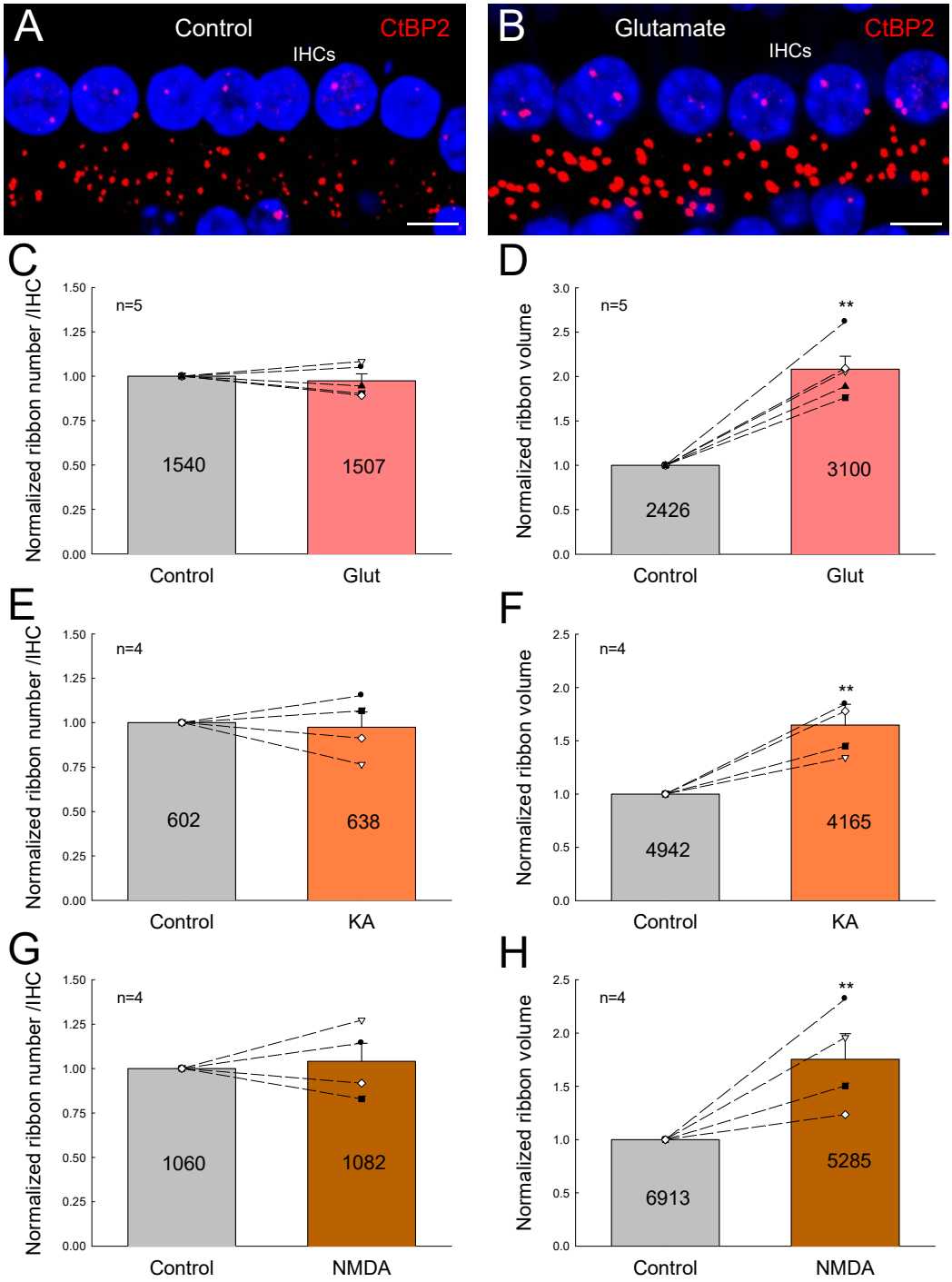

Fig 4. Glutamate and glutamate receptor agonists can cause ribbon swelling but not degeneration

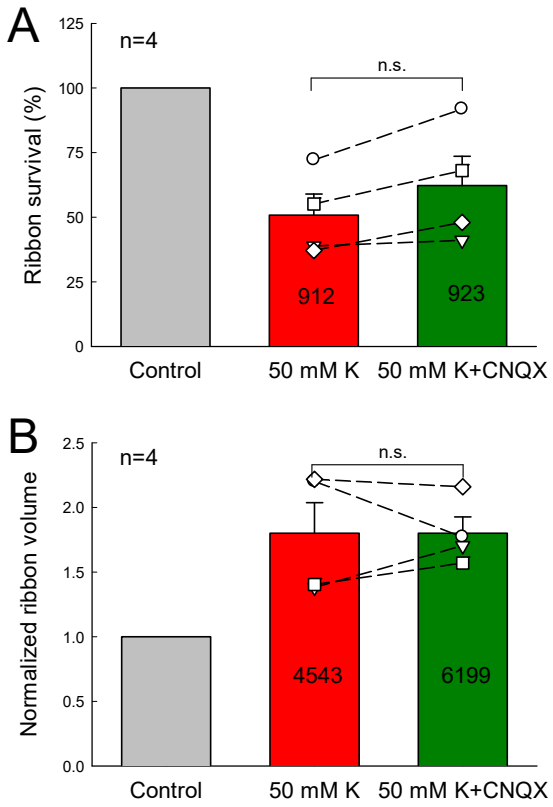

Fig 5. Glutamate receptor antagonist cannot eliminate K^+-induced ribbon degeneration and swelling

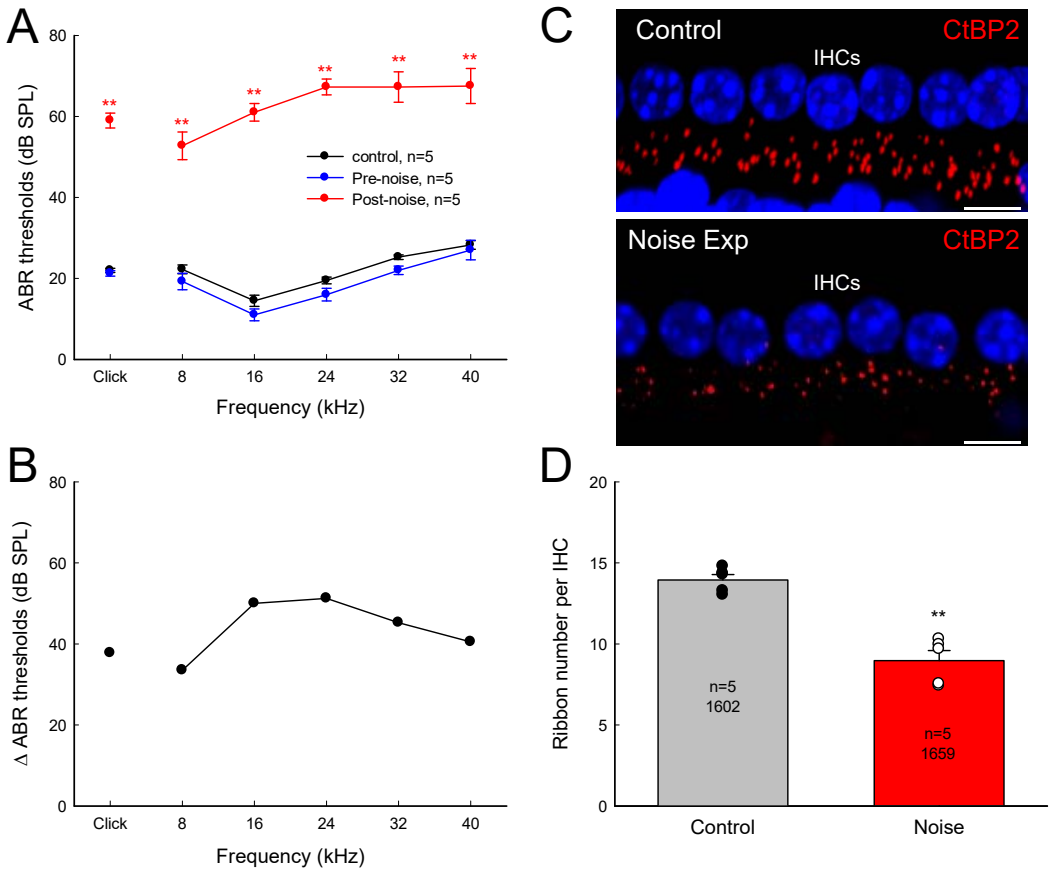

Fig 6. Noise-induced temporal threshold shift in hearing and IHC ribbon degeneration

Supplementary Materials

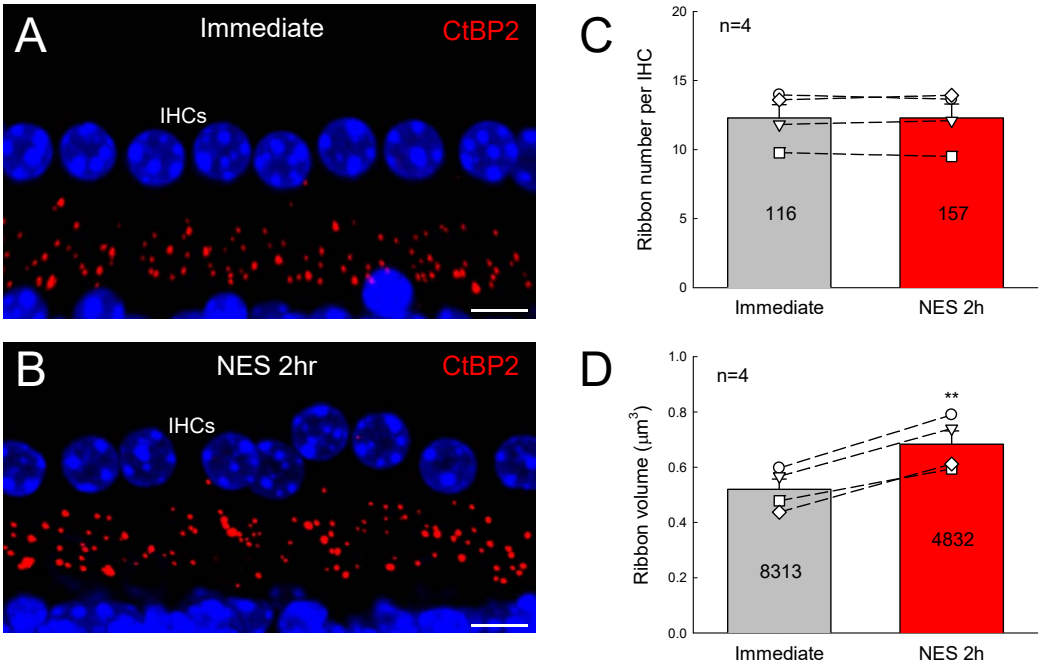

Fig. S1. Incubation procedure does not produce ribbon degeneration. One inner ear in a mouse was immediately fixed after isolation and stained for CtBP2, while another inner ear in the same mouse was incubated in NES for 2 hr and then fixed for staining. A-B: Immunofluorescent staining for CtBP2 in the immediate control group and NES-incubation group. Scale bar = 10 μm. C-D: Quantitative analysis of ribbon numbers and volumes. Dashed line connections represent data collected from two inner ears in the same mouse. Data were collected from 4 mice. Numbers in the bars represent the total numbers of accounted IHCs and measured ribbons. There is no significant ribbon degeneration after incubation in NES for 2 hr (panel C). However, ribbon volumes in the incubation group are significantly increased (panel D). **: $P < 0.01$, paired t test, two-tail.

Supplementary Materials

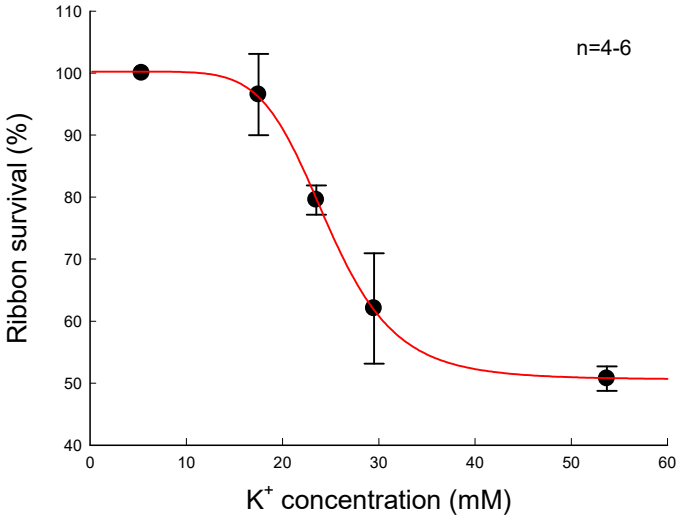

Fig S2. Dose-curve of ribbon degeneration in IHCs by K^+. A smooth solid line represents data fitting to a Hill's function $y=y_0+a*C^n/(EC_{50}^n+C^n)$, where median concentration EC_{50}=24.7 mM .

Supplementary Materials

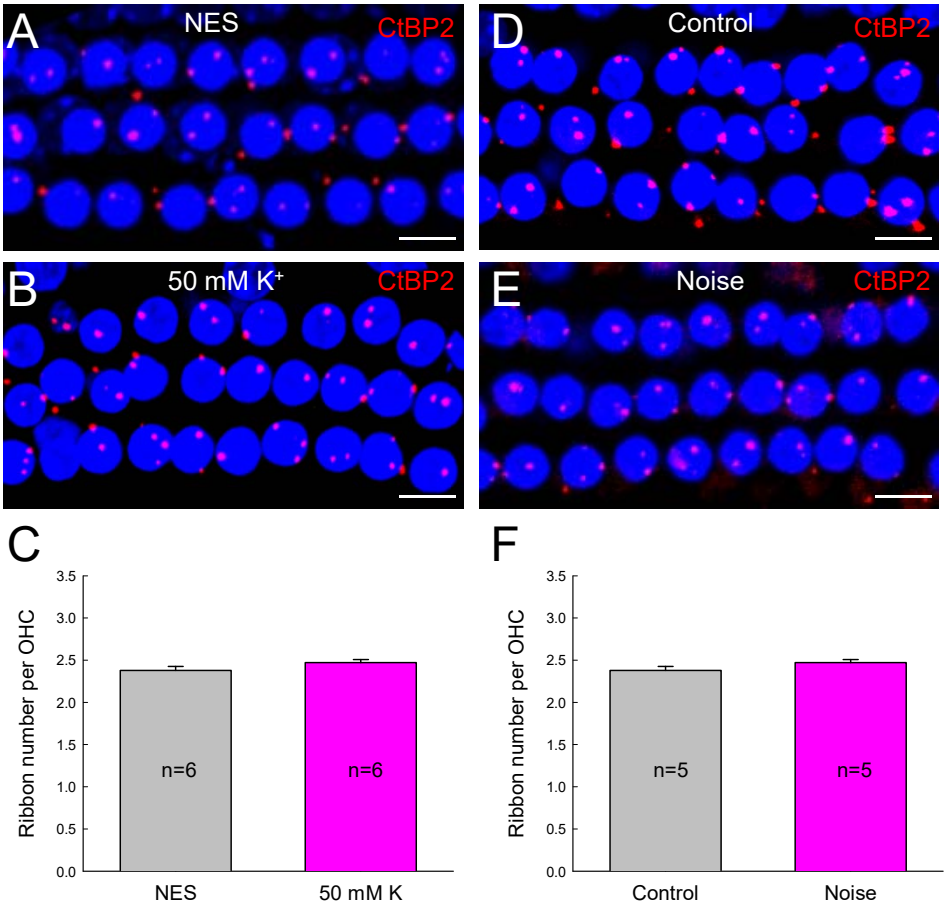

Fig. S3. No OHC ribbon synapse degeneration by high-K^+ challenge and noise exposure. No significant ribbon degeneration in outer hair cells (OHCs) for high K^+ challenge and noise exposure. A-B: Immunofluorescent staining for CtBP2 in OHC area for high-K^+ treatment. C: There is no significant degeneration of OHC ribbon synapses for high-K^+ challenge (P=0.31, pared t test, two-tail). D-E: Immunofluorescent staining for CtBP2 in OHC area after noise exposure. F: There is no difference of ribbon synapses in OHCs between noise-exposure group and control group (P=0.25, t test, two-tail). Scale bar = 10 μm.